ACSNANO

www.acsnano.org

ARTICLE

Scaling Laws in the Diffusive Release of Neutral Cargo from Hollow Hydrogel Nanoparticles: Paclitaxel-Loaded Poly(4-vinylpyridine)

Arturo Moncho-Jordá,* Ana B. Jódar-Reyes, Matej Kanduč, Alicia Germán-Bellod, Juan M. López-Romero, Rafael Contreras-Cáceres, Francisco Sarabia, Miguel García-Castro, Héctor A. Pérez-Ramírez, and Gerardo Odriozola*

Cite This: https://dx.doi.org/10.1021/acsnano.0c05480

Read Online

ACCESS | Metrics & More | Article Recommendations | Supporting Information

ABSTRACT: We study the nonequilibrium diffusive release of electroneutral molecular cargo encapsulated inside hollow hydrogel nanoparticles. We propose a theoretical model that includes osmotic, steric, and short-range polymer−cargo attractions to determine the effective cargo−hydrogel interaction, u_{eff}*, and the effective diffusion coefficient of the cargo inside the polymer network, D_{eff}*. Using dynamical density functional theory (DDFT), we investigate the scaling of the characteristic release time, $\tau_{1/2}$, with the key parameters involved in the process, namely, u_{eff}*, D_{eff}*, and the swelling ratio. This effort represents a full study of the problem, covering a broad range of cargo sizes and providing predictions for repulsive and attractive polymer shells. Our calculations show that the release time through repulsive polymer networks scales with $q^2e^{\beta u_{eff}*}/D_{eff}$* for βu_{eff}* ≫ 1. In this case, the cargo molecules are excluded from the shell of the hydrogel. For attractive shells, the polymer retains the cargo molecules on its internal surface and its interior, and the release time grows exponentially with the attraction strength. The DDFT calculations are compared to an analytical model for the mean first passage time, which provides an excellent quantitative description of the kinetics for both repulsive and attractive shells without fitting parameters. Finally, we apply the method to reproduce experimental results on the release of paclitaxel from hollow poly(4-vinylpyridine) nanoparticles and find that the slow release of the drug can be explained in terms of the strong binding attraction between the drug and the polymer.

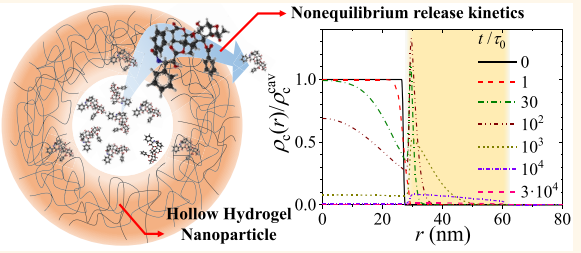

KEYWORDS: *hollow hydrogel, molecular cargo, dynamical density functional theory, diffusive release, kinetics, paclitaxel, poly(4-vinylpyridine)*

A gel is a three-dimensional cross-linked polymer network immersed in a fluid, which is most often water.[1] Nowadays, these polymeric systems have attracted considerable attention in a large number of scientific and technological fields, such as nanotechnology, materials science, life sciences, and medicine.[2] They have been applied in surface coating,[3] drug accumulation and release,[4] drug delivery,[5−7] optoelectronic switches,[8] and many other applications. Among them, stimuli-responsive (smart) nanogels (gels with dimensions in the nanometer range) undergo a sharp and reversible volume phase transition (a conformational change that leads to a drastic variation in the degree of swelling) in a response to environmental stimuli, such as the change in temperature,[9] pH,[10] ionic strength,[11] or solvent nature.[12] These properties made them particularly interesting for various nanotechnological and nanomedicinal applications as nanocarriers for different types of molecules (drugs, reactants, proteins), such as drug delivery, in chemical separation and catalytic processes.[13−15]

Two of the more investigated hydrogels in colloidal chemistry are made of poly(*N*-isopropylacrylamide) (pNIPAM) and poly(4-vinylpyridine) (p4VP).[16−19] These nanoparticles pos-

Received: July 2, 2020
Accepted: October 30, 2020

sess thermo- and pH-responsive capabilities, respectively. The former has the volume phase transition temperature at about 32 °C, and the latter has the phase transition at pH 4.8.

For certain applications (*e.g.*, drug delivery), nanogels are fabricated with a hollow cavity in the center, which—while maintaining the responsiveness—improves the loading capacity and the accumulation of molecules such as polysaccharides, enzymes, nucleic acids, or cells.[20−25] This preserves the biological activity of the biomolecules, reduces their toxicity, and protects them from enzymatic or chemical degradation. For instance, hollow p4VP hydrogels have recently been used to encapsulate molecules of paclitaxel (one of the most efficient cytotoxins for the treatment of lung and breast cancer), improving antitumor activity and reducing side effects in *in vivo* experiments.[26]

The design of optimal nanocarriers relies on extensive experimental work and is currently mostly based on trial and error.[27] To assist the development of rational designing of responsive nanogels, we need reliable theoretical models, which can predict the behavior of these particles as a function of observable parameters. For instance, the modeling of the kinetics of cargo encapsulation and release processes is fundamental to optimize the efficiency of these nanoparticles.

There are two descriptors used in physical sciences and material engineering that determine the kinetics of cargo molecules through complex media, such as a polymer network of a hydrogel nanoparticle. The first one is the partition coefficient, K, defined as the ratio of the equilibrium concentrations of the molecules inside and outside the medium. For diluted suspensions, the partition coefficient may be expressed as $K = e^{-\beta u_{eff}*}$. Here, $\beta = 1/(k_B T)$ (T is the absolute temperature and k_B the Boltzmann constant), and $u_{eff}*$ is the free energy difference of inserting a single cargo molecule inside the medium from the bulk solution. The second one is the effective diffusion coefficient of the penetrating molecules inside the given medium, $D_{eff}*$. A complete theory aimed to describe the encapsulation/release process should first provide a proper estimation of $u_{eff}*$ and $D_{eff}*$ and then be able to consider both parameters in the governing kinetic equations.

Nowadays, the most popular models are based on the ideal diffusion equation.[28−30] However, in those models the polymer−drug interaction is not explicitly considered. Some authors deal with the kinetics as a generalized diffusion equation, including the activity of the components of the system.[31] Recently, a model for the encapsulation kinetics of charged and dipolar cargo molecules in charged hollow hydrogels based on dynamic density functional theory (DDFT) has been developed, which combines a phenomenological effective cargo−hydrogel interaction potential and their effects on the effective cargo diffusion coefficient inside the polymer network.[32,33] It is well known that excluded-volume effects induced by the polymer give rise to a repulsive free energy barrier that the cargo molecules need to overcome to diffuse through. In this case, the cargo molecules are simply excluded from the polymer shell. In addition, the steric obstruction also reduces the diffusion coefficient of the molecules across the polymer network.[34−36] However, these theoretical models predict times for diffusive release from hydrogels below milliseconds, which are many orders of magnitude smaller than some experimentally observed time scales on the order of minutes,[37] hours, or days, even for hydrogel particles in the swollen state.[26]

As we elaborate in this study, the explanation for this huge mismatch relies on the existence of an intense attraction between the cargo molecules and the polymer chains. The attraction leads to the retention of the cargo inside the hydrogel shell. Furthermore, a high local cargo concentration at the internal interface may even produce the blockage of the paths for other molecules still in the cavity of the hydrogel. The origin of the short−range attraction could be hydrophobic (as in the case of paclitaxel trapped inside hollow-p4VP[26]), hydrogen bonding (as reported for isoniazid (INH), an antitubercular drug, loaded into PNIPAM-based hollow nanogels[37]), van der Waals,[38] or more complex, such as the one induced by supramolecular π-stacking effects.[39] To address the diffusive release through attractive polymer networks, we need to expand the theoretical model to incorporate a short-range cargo−polymer attraction in the expressions of $u_{eff}*$ and $D_{eff}*$, which represents the first goal of this work. This is shown in detail in the Methods section.

On the basis of this model, we explore the characteristic release time and analyze its scaling with all the relevant parameters involved in this problem, namely, the total effective interaction between the cargo molecule and the polymer, $u_{eff}*$, the diffusion coefficient of the specific substance inside the polymer network, $D_{eff}*$, and the swollen state of the hydrogel, q.

In the Results and Discussion section, we start by briefly introducing the model and the necessary concepts to expose our main findings. Then, we obtain general theoretical predictions regarding the scaling of typical release times with the different parameters and deduce an analytical model (derived from the mean first passage time integral equation[40]) to organize all these results into a global scaling expression. These scaling laws are used to interpret the experimental data and to estimate the attraction strength required to explain the large release times of paclitaxel encapsulated in hollow-p4VP observed in the experiments. Our improved theoretical model offers further insights into the release kinetics, which are crucial for the rational design of nanocarriers. Also, it enables good estimates without extremely time-consuming theoretical calculations in release processes that experimentally take hours or days. The derivation of the effective cargo−hydrogel interaction, $u_{eff}*$, in terms of the osmotic, steric, and short-range attractive contributions is performed in the Methods section. There, we also deduce an expression for $D_{eff}*$ as a function of the attractive contribution. The DDFT employed to calculate the (out-of-equilibrium) time evolution of the cargo density profile is explained in the Supporting Information (SI).

RESULTS AND DISCUSSION

To theoretically investigate the release of neutral encapsulated cargo inside a hollow hydrogel nanoparticle, we develop expressions for $u_{eff}*$ and $D_{eff}*$ that take the osmotic, excluded-volume, and attractive binding effects into account. These two quantities, together with the hydrogel swollen state, are the leading parameters controlling the release process. We use them to calculate the nonequilibrium time evolution of the cargo concentration using the DDFT. Then, we investigate the scaling and deduce a practical analytical expression for the mean release time in terms of these three parameters. Finally, we apply these theoretical predictions to explain the slow release of paclitaxel molecules from hollow p4VP hydrogel nanoparticles observed experimentally.

In order to achieve these goals, we consider a single ionic (pH-dependent) hollow hydrogel particle immersed in an aqueous solution of monovalent salt with concentration $\rho_s = 0.15$ M at room temperature. Ions are assumed to be point-like, and water is treated as a uniform background of relative permittivity $\epsilon_r =$

https://dx.doi.org/10.1021/acsnano.0c05480
ACS Nano XXXX, XXX, XXX−XXX

78.5. The hydrogel particle is modeled by a hollow sphere with an internal and external radius a and b, respectively (see Figure 1). The polymer volume fraction, $\phi_p(r)$, is assumed to be

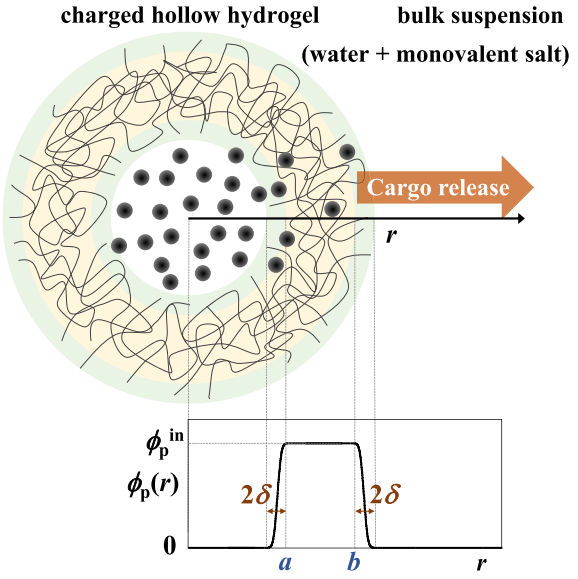

Figure 1. Illustration of the release process of electroneutral cargo molecules encapsulated inside a hollow hydrogel particle. The radial dependence of the polymer volume fraction given by eq 1 is also shown at the bottom of the figure.

uniform inside the polymer shell and goes to zero at the internal and external interfaces. We model this radial dependence by combining two error functions (see $\phi_p(r)$ at the bottom of Figure 1), so $\phi_p(r) = \phi_p^{in} g(r)$, with

$$g(r) = \frac{1}{2}[\mathrm{erf}(2(r - R_1)/\delta) - \mathrm{erf}(2(r - R_2)/\delta)] \quad (1)$$

where r is the distance to the center of the particle, ϕ_p^{in} is the polymer volume fraction inside the spherical shell, 2δ represents the thickness of the internal and external interfaces, and $R_1 = a - \delta$ and $R_2 = b + \delta$. In the initial state, the particle contains a molecular compound of concentration ρ_c^{cav} inside its cavity.

Figure 1 illustrates schematically the release process and the distribution of polymer mass inside the hydrogel particle. The charge density of the hydrogel is assumed to follow the same profile as the polymer volume fraction, *i.e.*, $\rho_m(r) = \rho_m^{in} g(r)$, where ρ_m^{in} is the concentration of charged monomers in the hydrogel shell. The polyelectrolyte network represents a charged background through which ions can diffuse. Since the polymer gel is homogeneous in space, so are all its properties, *e.g.*, polymer volume fraction, Donnan potential, and the local diffusion coefficient. These properties decay from that of the gel to their value in the bulk solution within an interface width given by 2δ.

The effective interaction between a single neutral cargo molecule and the hydrogel, $u_{eff}(r)$, is the transfer free energy of the cargo molecule from the bulk suspension to a distance r from the hydrogel center. Inside the uniform region of the polymer gel, we denote its value as u_{eff}^*. It can be written as

$$u_{eff}(r) = u_{osm}(r) + u_{ster\text{-}att}(r) \quad (2)$$

Here, $u_{osm}(r)$ is the work against the osmotic pressure exerted by the mobile ions onto the cargo molecule inside the hydrogel network. As a consequence of the counterion excess inside the charged hydrogel nanoparticle, the osmotic contribution always has the form of a repulsive energy barrier, which hinders the penetration of cargo inside the polymer shell. The second term, $u_{ster-att}(r)$, incorporates the interplay between the excluded volume (steric) repulsion and the attractive binding of the cargo to the polymer chains. The steric repulsion depends on the characteristic size of the monomers and cargo molecules (denoted by R_m and R_c, respectively) and grows when increasing the polymer volume fraction $\phi_p(r)$.

To provide a general theoretical description, we make no further assumptions on the specific nature of this attraction. We only consider it to act in a small vicinity of the polymer chain (short-range interaction) and denote its strength and range by ϵ and Δ, respectively. The steric repulsion and the attractive binding compete to determine the cargo partition coefficient, K. If the volume exclusion effect induced by the polymer chains dominates, the hydrogel shell repels the cargo molecule. Conversely, if the binding attraction is sufficiently large, $u_{ster-att}(r)$ takes the form of a potential well that attracts the cargo inside the shell, leading to its retention. Whether the repulsion or attraction dominates depends on the model parameters ($\phi_p(r)$, R_m, R_c, ϵ, and Δ). In the Methods section, we deduce a general analytical expression for $u_{eff}(r)$ and discuss its validity (see eqs 7 and 10).

The effective diffusion coefficient, $D_{eff}(r)$, also depends on the location of the cargo molecule. Inside the cavity and outside the hydrogel it is given by the bulk diffusion coefficient, D_0. Inside the uniform polymer shell, $D_{eff}(r)$ is denoted by D_{eff}^*. The diffusion coefficient changes continuously from D_0 to D_{eff}^* at both interfaces of the polymer shell. In general, D_{eff}^* is smaller than D_0 due to the effect of the cross-linked polymer network, which restricts the accessible volume for the cargo and enhances the hydrodynamic drag. In addition, the presence of a short-range binding attraction between the cargo molecules and the polymer chains leads to their retention at the binding sites, decreasing even more the cargo diffusivity. In the Methods section, we provide an analytical expression for $D_{eff}(r)$ that considers all these effects. These are given by eqs 13 and 15 (for nonattractive and attractive polymer shells, respectively). We also show that the cargo diffusivity is controlled by the "roughness" of the energy landscape inside the attractive polymer network. For specific compounds and thermodynamic conditions, it is possible to access $K = e^{-\beta u_{eff}^*}$ and D_{eff}^* through atomistic computer simulations.[38,41−45]

The degree of swelling of the hydrogel, q, is defined as the ratio between the radius of the particle, b, and the one in the collapsed state, b_0, $q = b/b_0$. Assuming uniform swelling, the other characteristic lengths and the polymer volume fraction are given by $a = qa_0$, $\delta = q\delta_0$, and $\phi_p^{in} = q^{-3}\phi_p^{in,0}$, where a_0, δ_0, and $\phi_p^{in,0}$ are the corresponding values in the collapsed state. We set $a_0 = 25$ nm and $b_0 = 50$ nm, which are the corresponding values for hollow-p4VP hydrogel nanoparticles used in the experiments of paclitaxel release described below. The interface thickness of the collapsed state is usually very narrow, about a few nanometers;[46] hence we assume $\delta_0 = 1$ nm. Even for collapsed hydrogels, the amount of water can be significant. Here, we assume a polymer volume fraction in the collapsed state of $\phi_p^{in,0} = 0.5$, as typically accepted in the literature.[46] For pH-responsive hydrogels, the particle swelling is controlled by the charge density, so $\rho_m^{in,0}$ is close to zero, and increases with lowering (raising) the pH for positively (negatively) charged hydrogels. We set $\rho_m^{in,0} = 0.4$ M, which again corresponds to the charge

https://dx.doi.org/10.1021/acsnano.0c05480
ACS Nano XXXX, XXX, XXX−XXX

density of the hollow nanoparticles used in the experiments. The effect of the steric exclusion is explored by varying the swelling ratio from $q = 1$ (collapsed) to $q = 3$ (swollen). We set $R_m = 0.35$ nm, which is a reasonable value for the radius of the monomeric units.[47,48]

The hydrogel nanoparticle contains inside a solution of neutral cargo molecules, modeled by hard spheres of radius R_c, described *via* a continuous time-dependent radial density profile $\rho_c(r, t)$. We consider electroneutral cargo molecules with a characteristic radius $R_c = 0.5-1.25$ nm to cover the sizes of different hydrophobic drugs involved in various therapeutic treatments, such as hydrocortisone, budesonide, dexamethasone, paclitaxel, tamoxifen, or β-lapachone.[26,49−51] At the initial stage, all cargo molecules are encapsulated inside the hydrogel's cavity. The initial concentration is given by $\rho_c^{cav} = 2 \times 10^{-4}$ M, which is the value used in the experimental part of this work. The typical time to diffuse along the distance $l_0 = 1$ nm, used to convert the real time into dimensionless time, is $\tau_0 = l_0^2/D_0$. As the release process takes place, the initially uniformly distributed cargo in the cavity progressively decreases until the total amount is delivered. At any time, the number of molecules encapsulated inside the hydrogel is obtained by integrating the density, $N(t) = 4\pi \int_0^{b+2\delta} \rho_c(r,t) r^2 \, dr$, from which the fraction of released cargo is $f_{rel}(t) = 1 - N(t)/N(0)$.

The theoretical framework employed to obtain the time evolution of the cargo concentration profile by means of DDFT is detailed in the SI.[52] This method not only takes into account the effective interaction and the reduced diffusion coefficient profile, but also the cargo−cargo interaction induced by volume exclusion effects, which may cause the blockage of the diffusive transport under particular conditions.

f2 Figure 2(a) illustrates the shape of the effective interaction induced by the hollow hydrogel onto the cargo molecule for two representative situations. This shape has strong implications on the kinetics of the cargo release. For $\beta u_{eff}^* = 2$, the interaction profile $u_{eff}(r)$ takes the form of a repulsive free energy barrier. Indeed, increasing the height of this barrier impedes the cargo penetration to the polymer matrix, decreasing the release rate. Conversely, for $\beta u_{eff}^* = -2$, the attraction between the cargo and the polymer chains leads to an effective potential that has the shape of an attractive well. In this case, the cargo molecules contained in the cavity are likely to diffuse inside the polymeric shell, where they tend to be retained. In both cases (repulsion and attraction), $u_{eff}(r)$ is flat inside the uniform polymeric gel.

The effect that the shape of $u_{eff}(r)$ has on the time-dependent release profiles may be clearly appreciated in Figures 2(b) and (c), which show illustrative examples of the time evolution of the normalized cargo concentration, $\rho_c(r)/\rho_c^{cav}$, for repulsive and attractive polymer shells, respectively. As observed, the time dependencies of the profiles are different in both situations. In the repulsive scenario, the cargo molecules repelled by the polymer network require some time to surpass the energy barrier at the internal interface ($r = a$). Once they diffuse inside the polymer network, the diffusive release process follows a quasi steady-state flow and the profiles are linear across the gel. Conversely, if the molecules are attracted to the polymer, they accumulate at the internal surface, leading to a pronounced sharp peak that builds up quickly and only slowly widens and diffuses toward the end of the gel, due to the reduced diffusion coefficient in this region. In this case, the density profile does not adopt a linear steady-state shape. Once the cargo molecules have diffused through the hydrogel, they still need to overcome the other barrier located at $r = b$ to escape from it. Note that there is

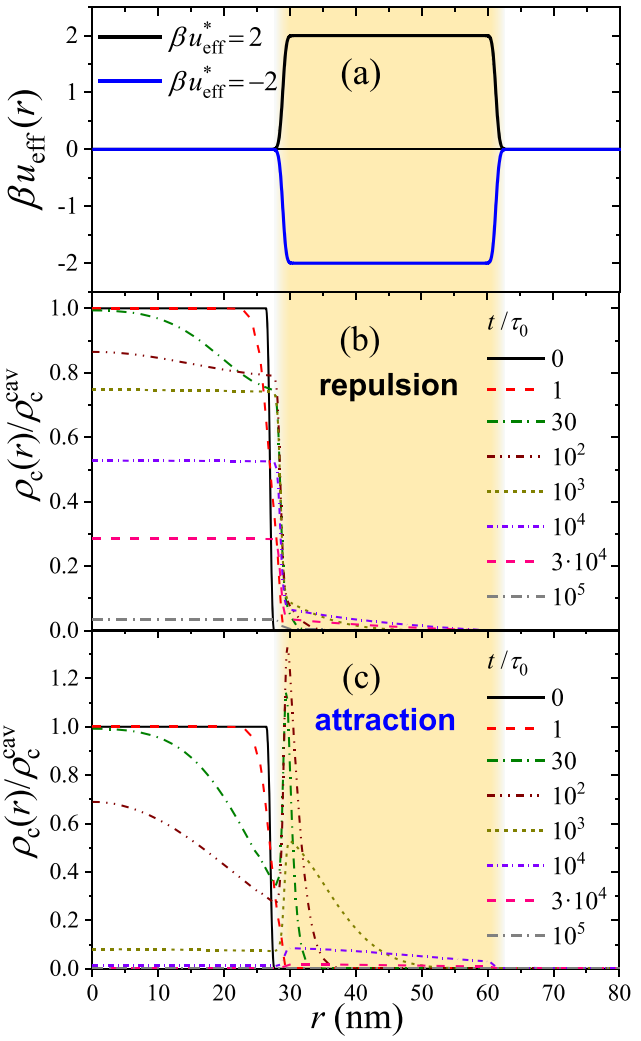

Figure 2. (a) Effective potential induced by the hydrogel for two particular cases: repulsive barrier ($\beta u_{eff}^* = 2$) and attractive well ($\beta u_{eff}^* = -2$). Plots (b) and (c) show the time evolution of the normalized cargo concentration for repulsive and attractive potentials shown in plot (a), respectively. In both cases $R_c = 0.5$ nm, $D_{eff}^*/D_0 = 0.038$, and $q = 1.2$. The colored region denotes the shell (internal cavity on the left and bulk suspension on the right).

a steep decrease of the cargo profile when passing through the outer interface, pointing out the difficulty that molecules experience to escape from the hydrogel. This effect, when enhanced by increasing the polymer−cargo attraction, leads to the retention of the molecules inside the hydrogel. Note also that the adsorption at the internal interface may even produce the blockage of the paths, reducing the transport. Here, the diffusion through the polymer shell controls the process, since the concentration peak at the inner interface tends to diminish its height, leaving room for more molecules to enter the polymer shell. Although the scenarios are quite different in the attractive and repulsive cases, in both situations the cargo release always involves overcoming an energy barrier and diffusing through the polymer matrix, which represents a region of a damped diffusion coefficient.

Scaling of the Characteristic Release Time. One of the main goals of this paper is to investigate the scaling of the cargo release rate as a function of the basic physical parameters of the system, namely, the effective hydrogel−cargo interaction, u_{eff}^*,

https://dx.doi.org/10.1021/acsnano.0c05480
ACS Nano XXXX, XXX, XXX−XXX

the diffusion coefficient inside the hydrogel, D_{eff}*, and the swelling ratio, q. For this purpose, we examine the behavior of $\tau_{1/2}$, defined as the time required to release half of the encapsulated cargo, with the above-mentioned physical parameters. The precise knowledge of the scaling of $\tau_{1/2}$ with u_{eff}*, D_{eff}*, and q is especially useful for the particular case of very slow release processes. The latter can occur in the presence of an intense excluded-volume repulsion or binding attraction between the cargo and the hydrogel, which leads to retention and reduced transport of the cargo molecule. The scaling behavior may be exploited to obtain reliable predictions in those regimes where the integration of the DDFT can involve prohibitively long calculations.

We first start varying the effective cargo−hydrogel repulsive barrier for a fixed D_{eff}*/D_0 = 1 and q = 1. Figure 3 shows the time

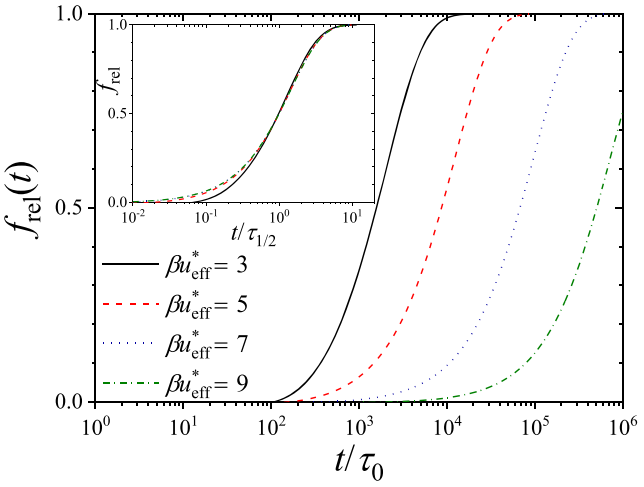

Figure 3. Time evolution of the fraction of released cargo for βu_{eff}* = 3, 5, 7, and 9. Inset: Fraction of released cargo, rescaled by $\tau_{1/2}$. In all cases D_{eff}*/D_0 = 1, q = 1, ρ_c^{cav} = 2 × 10^{-4} M, and $\rho_m^{in,0}$ = 0.4 M.

dependence of the fraction of released cargo for different u_{eff}* values. As observed, increasing the repulsion slows the release rate, even by several orders of magnitude. Basically, cargo molecules need to overcome a thermodynamic free energy barrier between the cavity and the polymer network. This process is strongly hindered when the height of this barrier increases. The inset in Figure 3 shows the same results but plotted against the scaled time, $t/\tau_{1/2}$. In this representation, a simple visual inspection of the curves demonstrates their collapse onto a single universal curve for βu_{eff}* > *rsim*4, which means that the kinetics follows a well-defined scaling behavior for large enough repulsion.

This scaling can be clearly appreciated in Figure 4(a), which plots $\tau_{1/2}$ as a function of βu_{eff}*. For small repulsions, βu_{eff}* $\lesssim$ 3, the release rate is controlled by many processes that contribute similarly: the diffusion inside the cavity, the diffusion across the polymer network, and the surpassing of the repulsive barrier. However, for βu_{eff}* > 3, the contribution of the energy barrier governs the kinetics over the other effects. In this regime, $\tau_{1/2}$ grows exponentially with the height of the repulsive barrier, following an Arrhenius law dependence, $\tau_{1/2} \sim e^{\beta u_{eff}*}$.

On the other hand, if u_{eff}* <0, the hydrogel shell behaves as a potential well for the incoming molecules so that they rapidly enter into the polymer network. However, they have to diffuse through the polymer shell and overcome the repulsive barrier at

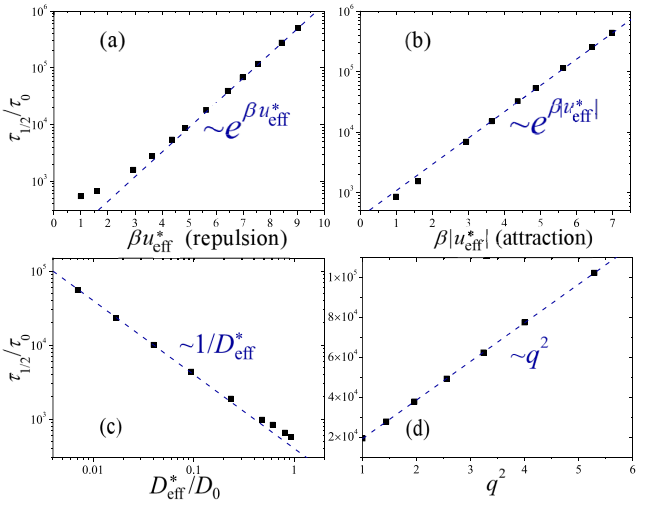

Figure 4. Scaling of $\tau_{1/2}$ with (a) the effective cargo−hydrogel repulsion, u_{eff}* (D_{eff}*/D_0 = 1 and q = 1), (b) the effective cargo−hydrogel attraction (D_{eff}*/D_0 = 1 and q = 1), (c) the effective diffusion coefficient inside the polymer shell (βu_{eff}* = 1 and q = 1), and (d) with the swelling ratio, q (βu_{eff}* = 1 and D_{eff}*/D_0 = 0.2). In all cases R_c = 1.25 nm, ρ_c^{cav} = 2 × 10^{-4} M, $\rho_m^{in,0}$ = 0.4 M, and ρ_s = 0.15 M.

$r = b$ to escape to the bulk solution. Figure 4(b) shows $\tau_{1/2}$ in the attractive case as a function of the depth of the potential well. Again, for attractions above around $\beta|u_{eff}$*| > 3, the release time scales exponentially as $\tau_{1/2} \sim e^{\beta|u_{eff}*|}$. This result can also be understood in terms of the Arrhenius law, where $|u_{eff}$*| represents the activation energy for the molecules to escape outside the attractive well.

The dependence of $\tau_{1/2}$ on the cargo diffusion coefficient inside the polymer network is plotted in Figure 4(c) for βu_{eff}* = 1 and q = 1. We clearly see that $\tau_{1/2} \sim 1/D_{eff}$* for small enough values of D_{eff}*. In this regime, the release is almost completely controlled by the diffusion time through the polymer shell, given by $(b-a)^2/(2D_{eff}*)$. As D_{eff}* approaches D_0, the results deviate from this scaling because other contributions come into play, such as the diffusion from the cavity to the internal interface and the surpassing of the repulsive barrier at $r = a$. Finally, in Figure 4(d) we examine the effect of the hydrogel thickness, where we depict $\tau_{1/2}$ as a function of the square of the swelling ratio, q^2, for βu_{eff}* =1, D_{eff}*/D_0 = 0.2, and ρ_c^{cav} = 2 × 10^{-4} M. The DDFT results perfectly agree with the scaling $\tau_{1/2} \sim q^2$ for the whole range of q values. This confirms that the cargo release is a diffusion-controlled process, so the average square distance traveled by the molecules grows linearly with time.

All these scaling laws suggest that it should be possible to derive a general expression to account for the whole process. In our case, the concentration of cargo molecules is low everywhere, such that cargo−cargo excluded-volume interactions are weak. Therefore, the release process can be modeled as a simple diffusion problem of molecules through the effective potential induced by the hydrogel, $u_{eff}(r)$.[53−55] In other words, we are interested in the time spent by the molecules initially distributed inside the cavity to reach the external surface of the hydrogel, located at $r > b + 2\delta$. Direct integration of the Smoluchowski equation leads to the following expression for the mean first passage time:[40]

https://dx.doi.org/10.1021/acsnano.0c05480
ACS Nano XXXX, XXX, XXX−XXX

$$\langle\tau\rangle = \int_s^{b+2\delta} \mathrm{d}r \frac{\mathrm{e}^{\beta u_{\mathrm{eff}}(r)}}{D_{\mathrm{eff}}(r) r^2} \int_0^r \mathrm{d}r' r'^2 \mathrm{e}^{-\beta u_{\mathrm{eff}}(r')} \quad (3)$$

where the integral limit s denotes the location of the center of mass of the molecules distributed inside the cavity at $t = 0$. We get $s = qs_0$, with $s_0 = 17.8$ nm for a cavity uniformly filled with cargo molecules. In order to perform the double integral and calculate $\langle\tau\rangle$, we replace the smooth surfaces of the hydrogel shell by sharp interfaces in eq 1, such that $u_{\mathrm{eff}}(r) = u_{\mathrm{eff}}{}^*$ for $a < r < b$, and $u_{\mathrm{eff}}(r) = 0$ elsewhere. Analogously, $D_{\mathrm{eff}}(r) = D_{\mathrm{eff}}{}^*$ for $a < r < b$ and $D_{\mathrm{eff}}(r) = D_0$ elsewhere. Inserting these two simple prescriptions into eq 3 and taking into account that $b = qb_0$, $a = qa_0$, $\delta = q\delta_0$, and $s = qs_0$, we obtain

$$\langle\tau\rangle = \frac{q^2}{6D_0}(a_0{}^2 - s_0{}^2) + \frac{q^2}{6D_{\mathrm{eff}}{}^*}\left(\frac{2a_0{}^2(b_0 - a_0)}{b_0}(e^{\beta u_{\mathrm{eff}}{}^*} - 1) + b_0{}^2 - a_0{}^2\right) + \frac{q^2}{6D_0}\left(\frac{4(b_0{}^3 - a_0{}^3)\delta_0}{(b_0 + 2\delta_0)b_0}(e^{-\beta u_{\mathrm{eff}}{}^*} - 1) + 4b_0\delta_0 + 4\delta_0{}^2\right) \quad (4)$$

As seen, the time scales as $\langle\tau\rangle \sim q^2$, in consistency with the DDFT results shown in Figure 4(d). For processes dominated by a very high repulsive energy barrier, $\beta u_{\mathrm{eff}}{}^* \gg 1$, the mean first passage is controlled by the exponential in the second term, $\langle\tau\rangle \sim \mathrm{e}^{\beta u_{\mathrm{eff}}{}^*}$. Conversely, for strong cargo−hydrogel attractions, $\beta u_{\mathrm{eff}}{}^* \ll -1$, the exponential in the third term plays the key role, leading to $\langle\tau\rangle \sim \mathrm{e}^{-\beta u_{\mathrm{eff}}{}^*} \sim \mathrm{e}^{|\beta u_{\mathrm{eff}}{}^*|}$. In addition, if the cargo diffusion coefficient is very small inside the polymer shell, we recover the scaling $\langle\tau\rangle \sim 1/D_{\mathrm{eff}}{}^*$. Therefore, eq 4 brings together all the scaling trends discussed in Figure 4, involved in the release of neutral molecules. In the following sections, we use this expression to physically interpret the DDFT calculations for repulsive and attractive polymer shells.

Release Kinetics through a Repulsive Polymer Shell. Given that all the relevant hydrogel parameters change with the degree of swelling, it is interesting to take a closer look at how cargo release time depends on it. We first start with repulsive polymer networks. The effective interaction $u_{\mathrm{eff}}(r) = u_{\mathrm{osm}}(r) + u_{\mathrm{ster}}(r)$ is given in the Methods section by eqs 7 and 8. The effective diffusion coefficient inside the polymer network due to steric exclusion effects is provided by eq 13. As seen in Figure 5 (symbols), the combination of both effects entails a very significant increase in the release time for the collapsed state, $q \to 1$. For extremely swollen states, $\tau_{1/2}$ experiences again a slight increase because the cargo has to travel a larger distance to escape from the hydrogel.

The analytical predictions from eq 4 are plotted as lines in Figure 5. In spite of the simplifications involved, they quantitatively agree with the DDFT calculations without the use of any fitting parameter. For weakly repulsive polymer shells, all three terms in eq 4 contribute similarly. However, for a moderate repulsion, the second term dominates, leading to the following scaling: $\langle\tau\rangle \sim q^2(k_1\mathrm{e}^{\beta u_{\mathrm{eff}}{}^*} + k_2)/D_{\mathrm{eff}}{}^*$. This last expression gathers the governing effects implied in the diffusive release through a repulsive polymer network. Indeed, the term $q^2k_1\mathrm{e}^{\beta u_{\mathrm{eff}}{}^*}/D_{\mathrm{eff}}{}^*$ accounts for the precluded diffusion time required for the cargo molecules contained in the internal void

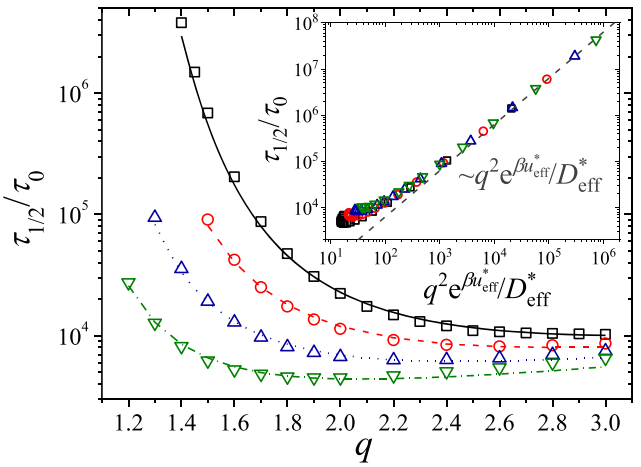

Figure 5. Symbols represent $\tau_{1/2}$ for neutral cargo molecules diffusing through a *repulsive* polymer shell of a hollow hydrogel as a function of the swelling ratio, q, for $R_c = 0.5$ nm (□), 0.75 nm (○), 1 nm (△), and 1.25 nm (▽). In all cases $\rho_c{}^{\mathrm{cav}} = 2 \times 10^{-4}$ M and $\rho_m{}^{\mathrm{in},0} = 0.4$ M. Lines correspond to theoretical predictions provided by eq 4. Inset: Asymptotic scaling of $\tau_{1/2}$ with $q^2\mathrm{e}^{\beta u_{\mathrm{eff}}{}^*}/D_{\mathrm{eff}}{}^*$.

to jump over the repulsive energy barrier and get into the polymer shell. The second term, $q^2k_2/D_{\mathrm{eff}}{}^*$, represents the necessary time for the cargo to diffuse over the hydrogel shell.

For nearly collapsed states, where $u_{\mathrm{eff}}{}^*$ is very large and $D_{\mathrm{eff}}{}^*$ very small, the second term in eq 4 dominates, which leads to the approximate expression

$$\langle\tau\rangle \sim q^2\mathrm{e}^{\beta u_{\mathrm{eff}}{}^*}/D_{\mathrm{eff}}{}^* \quad (5)$$

This result is consistent with the well-known Kramers escape time over a repulsive energy barrier through the shuttling action of thermal Brownian motion.[53,56] The inset of Figure 5 clearly shows that this scaling describes the release kinetics for this particular regime.

In materials science, the ability of different solutes to permeate through a membrane is quantified by the permeability, P. Based on the solution−diffusion theory,[57−61] the permeability is the product of the diffusion coefficient and the partition ratio in the membrane, $P = KD_{\mathrm{eff}}{}^*$. For diluted cargo suspensions, the partition coefficient can be approximated by $K = \mathrm{e}^{-\beta u_{\mathrm{eff}}{}^*}$, so the scaling given by eq 5 may be expressed as $\langle\tau\rangle \sim q^2/P$. Thus, the release time is controlled by the membrane permeability, which is an expected result since entering into the membrane is the rate-limiting step, so the release time in the case of a repulsive shell is inversely proportional to the flux (and thus the permeability) through the membrane.

Release Kinetics through an Attractive Polymer Shell. For attractive shells, the passing from the cavity toward the polymer network is a fast process, but as soon as the molecules have entered the polymer network, they have to diffuse through the shell and then overcome the positive energy difference on the external side of the hydrogel to escape. In fact, it is in the polymer shell where the molecules remain trapped for a longer time due to two reasons: the reduced diffusion and the retention induced by the energy barrier located at the outer interface.

We systematically study the role of the attraction by repeating the same calculations as the ones shown in Figure 5 at the same conditions, but replacing the repulsive interaction by an attraction given by $u_{\mathrm{eff}}(r) = -(u_{\mathrm{osm}}(r) + u_{\mathrm{ster}}(r))$. Results for the four studied cargo sizes are shown as symbols in Figure 6. As

https://dx.doi.org/10.1021/acsnano.0c05480
ACS Nano XXXX, XXX, XXX−XXX

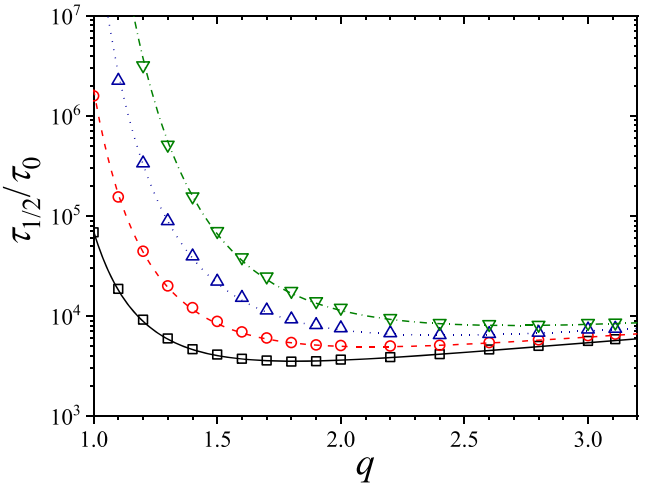

Figure 6. Symbols represent $\tau_{1/2}$ for neutral cargo molecules diffusing through an *attractive* polymer shell of a hollow hydrogel as a function of the swelling ratio, q, for R_c = 0.5 nm (□), 0.75 nm (○), 1 nm (△), and 1.25 nm (▽). In all cases $\rho_c^{cav} = 2 \times 10^{-4}$ M and $\rho_m^{in,0}$ = 0.4 M. Lines correspond to theoretical predictions provided by eq 4.

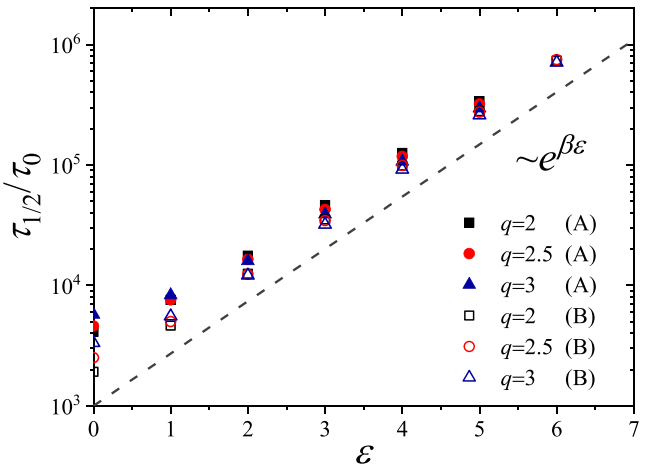

Figure 7. Symbols represent $\tau_{1/2}$ for neutral molecules diffusing through an attractive hollow hydrogel as a function of the cargo−polymer attraction strength ϵ for q = 2 (□), q = 2.5 (○), and q = 3 (△). In all cases, R_c = 0.575 nm (the mean size of the paclitaxel molecule), Δ = 1 nm, and $\rho_c^{cav} = 2 \times 10^{-4}$ M. Case (A): Solid symbols are the results assuming that cargo molecules are initially confined inside the cavity of the hydrogel. Case (B): Hollow symbols assume that the molecules are initially trapped in the polymer shell.

observed, the trends obtained for attractive molecules are very similar to the results deduced for repulsive ones. The reason for this similarity lies in the fact that, in both cases, the diffusion of the cargo molecules involves surpassing an energy barrier (located at $r = a$ for repulsive polymer shells and at $r = b$ for attractive ones).

As it can be observed from eq 4, the terms that scale with $1/D_0$ or $e^{\beta u_{eff}^*}$ are negligible compared to the others for strong attractions, and the release time is led by

$$\langle \tau \rangle \sim q^2 (k_1' e^{|\beta u_{eff}^*|}/D_0 + k_2'/D_{eff}^*) \quad (6)$$

The first term represents the typical time employed to escape from the energy barrier located at $b + 2\delta$, which defines the limit of the attractive well. The second term is the typical time required to diffuse through the polymer shell with a reduced diffusion constant D_{eff}^*. It is important to emphasize here that the scaling for an attractive shell is significantly different than for a repulsive one. Indeed, $\langle \tau \rangle$ does not scale inversely with the permeability.

To further explore the attractive case, we calculate $\tau_{1/2}$ as a function of the attraction strength between the cargo molecules and the polymer chains, $\beta\epsilon$. Here, ϵ is the depth of the square well potential function defined by eq 9 (see the Methods section). We set R_c = 0.575 nm, which is the characteristic size of the paclitaxel drug. The range of the attraction is chosen to be Δ = 1 nm, as hydrophobic interactions are typically in the range of the molecule size.[62,63] We restrict our calculations to swollen states above $q > 2$ to avoid the superposition of multiple attractions from many polymer chains. Solid symbols in Figure 7 depict $\tau_{1/2}(\epsilon)$ for three different swelling ratios. The DDFT calculations were performed using the effective interaction and diffusion coefficient for attractive cargo molecules provided in the Methods section by eqs 10 and 15, respectively. As expected, the release through a more collapsed hydrogel is slower for the same ϵ due to the reduction of the cargo diffusivity inside the polymer network. For small ϵ, the effective cargo−hydrogel interaction is still repulsive due to the steric exclusion effects, but eventually the release becomes controlled by the attraction for large ϵ. In the limit of very large attraction strengths, $\beta\epsilon \gg 1$, the effective interaction scales as $e^{\beta|u_{eff}^*|} \sim e^{\beta\epsilon}$, whereas $D_{eff}^* \sim e^{-\beta\epsilon}$, so eq 4 leads to the asymptotic behavior $\tau_{1/2} \sim e^{\beta\epsilon}$ for large ϵ, as shown in Figure 7. Therefore, $\tau_{1/2}$ experiences a very strong exponential increase with ϵ that entails a significant slowdown of the kinetics through attractive polymer shells.

Finally, it should be emphasized that all the scaling trends obtained before assume that the cargo molecules are initially confined at the cavity of the hydrogel. However, for attractive cargo molecules, we could expect part of them initially bound to the polymer network. In such a case, the cargo release should be faster and the shape of $f_{rel}(t)$ should be different. To account for this situation, we performed additional calculations in which the cargo concentration is distributed uniformly inside the polymer shell, so $\rho_c(r)$ = 0.2 mM for $a < r < b$ and $\rho_c(r) = 0$ elsewhere. The results, shown in Figure 7 by hollow symbols, confirm that the release process is faster when the cargo is trapped in the polymer shell since the average distance required to escape outside is shorter. In spite of this difference, the scaling $\tau_{1/2} \sim e^{\beta\epsilon}$ holds, as the cargo still needs to diffuse through the polymer network and overcome the attractive well at $r = b$.

Comparison to Experimental Data. Paclitaxel is one of the most effective cytotoxins for the treatment of breast and lung cancer, but its usage is limited by its low solubility, severe side effects, and low tumor selectivity.[64] Recent experiments have shown that encapsulating paclitaxel molecules inside nano-containers such as hollow hydrogels enhances its solubility, reduces its side effects, and enables the preferential delivery of the drug. Here, we apply our theoretical method to elucidate the release kinetics of a recent experiment where paclitaxel molecules were encapsulated inside pH-responsive hollow hydrogels.[26] Those hollow particles were prepared by oxidizing gold cores in a previously synthesized Au@p4VP system.

The free diffusion coefficient of paclitaxel molecules in water at room temperature is $D_0 = 4.27 \times 10^{-10}$ m^2/s.[65] From this, the hydrodynamic radius of the paclitaxel molecule can be obtained *via* the Stokes−Einstein relation $R_c = k_B T/(6\pi\eta D_0) \approx 0.575$ nm

https://dx.doi.org/10.1021/acsnano.0c05480
ACS Nano XXXX, XXX, XXX−XXX

(where T = 298 K is the temperature and $\eta = 8.9 \times 10^{-4}$ Pa·s is the water viscosity). This D_0 value leads to $\tau_0 = 2.34 \times 10^{-9}$ s.

On the other hand, p4VP is a pH-responsive hydrogel with swelling−deswelling capabilities. That is, its swelling depends on the local proton concentration. At pH 2, the pyridine located within the polymer network is protonated. Consequently, there appears a high electrostatic repulsion between the positive charges resulting in the microgel swelling. As the pH of the solution increases, deprotonation of the pyridine groups causes the p4VP to collapse due to the attractive hydrophobic forces between 4VP monomers. This property has been exploited to achieve the effective and stable incorporation of paclitaxel into the hollow p4VP nanoparticles. At pH 7.5, the polymer shell is completely collapsed ($\phi_p \approx 0.5$), with internal and external radii of a_0 = 25 nm and b_0 = 50 nm, so the diffusion of the paclitaxel molecules through the pores of the polymer network is strongly hindered by the steric exclusion. In the swollen state, the particle hydrodynamic radius becomes b = 155 nm at pH 3.5 (*i.e.*, a swelling ratio of q = 3.11). Inverting the data of electrophoretic mobility through the theory by Ohshima[66] leads to a number density of charged groups inside the polymer network of about $\rho_m^{in} \approx 0.4$ M. Under this situation, the cargo release is favored, within a characteristic time of about $\tau_{1/2} \approx 0.5$ days.

Paclitaxel molecules were encapsulated by adding the drug to a hollow-p4VP dispersion in water (3 mL, containing 3 mg of hollow particles, and 0.5 mg of paclitaxel). After 30 min under stirring, the mixture was sonicated for 5 min at 20 °C, and then the pH of the dispersion was reduced by adding 0.1 M HCl (approximately 200 μL). In this swollen state, paclitaxel molecules are able to diffuse through the nanogel network. After slow stirring for 30 min, an aqueous 0.1 M solution of NaOH (200 μL) was added. This pH increase results in deprotonation of the pyridine groups and causes the hollow-p4VP microgels to undergo hydrophobic collapse from a swollen to a nearly solvent-free state of the pyridine moieties. The final concentration of paclitaxel captured inside the hydrogel was estimated to be about ρ_c^{cav} = 0.2 mM.

As frequently done in a typical experiment of drug release, a sample of paclitaxel@p4VP complex (3 mg) was suspended in a citrate buffer solution (5 mL, pH 3.5) containing 0.1% Tween 80. Surfactant was used to increase the wettability of the microgel obtained after centrifugation and to improve the paclitaxel solubility. The tubes were placed in a water bath at 37 °C, with shaking at 100 rpm. At specific intervals, the medium containing the drug was transferred out and extracted with chloroform (3 × 3 mL). The final salt concentration of the suspension was ρ_s = 0.15 M. Fresh medium (5 mL) was added to the test tube for the continuous-release studies. The extracted sample was analyzed by high-performance liquid chromatography. More details about these experiments can be found in ref 26.

Square symbols in Figure 8 show the experimental results of the release of paclitaxel molecules encapsulated inside the above-described hollow hydrogels. As already mentioned, a surprising outcome is the slow kinetics observed even for swollen hydrogels. The release times $\tau_{1/2}$ are on the order of days, which are much larger than the calculated typical times of diffusion across swollen nonattractive polymer shells of the same size. These are of the order of 10^{-5} s! This points out the existence of an intense binding attraction, ϵ, between the paclitaxel molecules and the p4VP polymer chains, therefore increasing the typical release times by around 9 orders of magnitude.

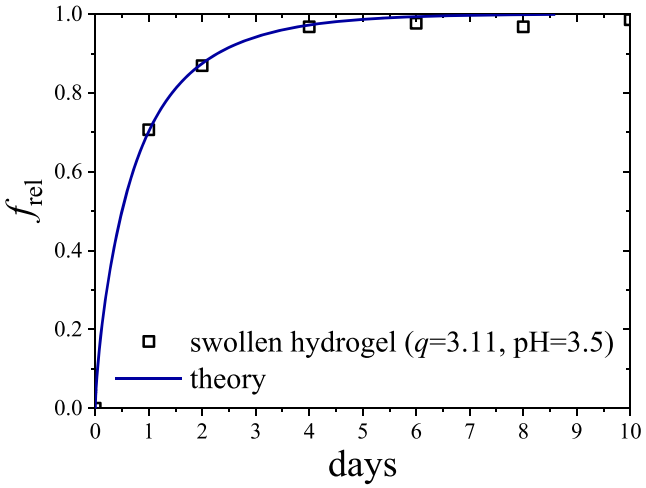

Figure 8. Fraction of released paclitaxel molecules from hollow p4VP hydrogels in the swollen state (□). The blue solid line is the theoretical fitting to the experimental data solving the DDFT equations and using the scaling $\tau_{1/2} \sim e^{\beta\epsilon}$, with ϵ as fitting parameter.

The density of charged groups inside the polymeric matrix for any swollen state is smaller than 0.4 M, for which the contribution of the osmotic term (eq 7) is negligibly small, $\beta u_{osm} \leq 0.07$. Hence, the effective interaction can be safely approximated by the steric−attractive term given by eq 10. In addition, the effective diffusion coefficient (eq 15) depends on ϵ. For very strong attraction we already showed that $\tau_{1/2} \sim e^{\beta\epsilon}$ (see Figure 7). Using this scaling behavior, the theoretical solution obtained with DDFT for small ϵ can be scaled to deduce the kinetics for very large ϵ. We followed this procedure to find the theoretical curve of $f_{rel}(t)$ that fits best the experimental data, shown as a solid line in Figure 8. As seen, the agreement is excellent. It is important to remark here that we assumed paclitaxel molecules to be initially contained in the polymeric shell. This is indeed a plausible hypothesis given the strong attraction between molecules and polymer chains.

The resulting fitting value is $\epsilon = 23.2 k_B T$ for pH 3.5 (swollen hydrogel). Therefore, paclitaxel molecules experience a very intense attraction to the p4VP chains, which justifies the slow release rates observed in the experiments. It would be interesting to compare this fitted value with the transfer free energy of the paclitaxel molecule from bulk water into the hydrogel. Unfortunately, to our knowledge, there is no such a computation in the literature. Nonetheless, transfer free energies of nonpolar molecules and big ions into pNIPAM hydrogel structures have been studied in detail.[44] The results show that they scale with the molecular surface area.[45] For shrunken states, where an adsorbing molecule exposes its complete surface to the polymer chains, the adsorption per surface area at 340 K is −18 kJ/mol/nm^2. Thus, we expect this number to decay to half its value for a swollen state, where an adsorbing molecule only exposes roughly half of its external surface to the polymer. The surface area of paclitaxel is around 7 nm^2,[67] which gives an estimate for pNIPAM−paclitaxel binding of $\epsilon = -22.3\ k_B T$. Since this binding is mainly of hydrophobic nature and thus molecule-unspecific, we can expect a similar value for the p4VP−paclitaxel binding. This estimate is very close to our fitted value for the depth of the attraction strength, despite the several assumptions and limitations of our model (see the SI). Given the good agreement with the experimental data, we believe that these approximations at least retain the fundamental physics to

https://dx.doi.org/10.1021/acsnano.0c05480
ACS Nano XXXX, XXX, XXX−XXX

understand the release process through attractive polymer membranes.

CONCLUSIONS

In this work, we used dynamical density functional theory to fully characterize the nonequilibrium diffusive release kinetics of neutral molecular cargo from a hollow spherical hydrogel carrier. We proposed a theoretical model that incorporates osmotic effects, the excluded-volume repulsion exerted by the polymer, and short-range cargo−polymer attractions (such us hydrophobic, hydrogen bonding, or van der Waals attractions). With this, we obtain analytical expressions for the partition coefficient, $K = e^{\beta u_{eff}^*}$, and for the effective diffusion coefficient, D_{eff}^*, of the cargo molecule inside the hydrogel. Despite the simplifications involved in both expressions, they show the right scaling behavior, in agreement with previously reported experimental and simulation data.

We focus on the scaling of the release time, $\tau_{1/2}$, with the key parameters involved in the process. These are the swelling ratio, q, the effective cargo−hydrogel interaction, u_{eff}^*, and the effective cargo diffusion coefficient inside the polymer network, D_{eff}^*.

We found that repulsive and attractive polymer shells lead to different scaling behavior of $\tau_{1/2}$. For repulsive polymer networks, $\tau_{1/2}$ is governed by two different events: overcoming the repulsive energy barrier at the internal interface of the hydrogel, and the attenuated diffusion through the polymer shell. In the limit of very strong repulsions, the density profiles are quasi-stationary and $\tau_{1/2}$ scales with the inverse of the permeability, $q^2 e^{\beta u_{eff}^*}/D_{eff}^* \sim q^2/P$. Conversely, the process across an attractive shell is slowed down by a high energy well at the external interface of the nanoparticle and, again, by the precluded diffusion through the polymer network. Both effects can drastically reduce the transport though the polymer shell. In addition, the second case can also lead to a blockage of the membrane for a sufficiently large initial cargo concentration. Our model naturally captures this possible effect through the cargo−cargo excluded volume interactions. In the limit of strong attractions, $\tau_{1/2}$ scales with the cargo−polymer attraction strength as $\tau_{1/2} \sim e^{\beta\epsilon}$, consistently with recent simulation data.[68]

We derived an analytical expression for the mean first passage time based on the Smoluchowski diffusion equation (eq 4). This theoretical prediction reproduces the whole set of DDFT results for repulsive and attractive shells without the use of fitting parameters. This equation can be used as a simple prescription to estimate the typical escape time of any neutral molecular cargo diffusing through a hollow hydrogel particle.

Finally, we applied our theoretical framework to reproduce the experiments on the release of paclitaxel drug from hollow p4VP hydrogel nanoparticles in the swollen state. The results show that the hydrophobic character of paclitaxel induces an intense attractive interaction between the drug and the polymer—on the order of $23k_BT$—which magnifies $\tau_{1/2}$ by around 9 orders of magnitude.

Future investigations will involve the study of concentrated and charged cargo suspensions. In this case, the effective diffusion coefficient becomes dependent on local cargo concentration. In addition, the saturation of the binding sites in attractive polymer networks can also entail consequences on the kinetics. We expect these conditions to activate the blockage of the polymer shell by increasing retention and reducing transport. This should yield even larger release times. In addition, we are also planning to perform atomistic simulations to determine K and D_{eff} for the paclitaxel molecule.

METHODS

Effective Hydrogel−Cosolute Interaction. The osmotic effect stems from the nonuniform distribution of counterions and co-ions that arises in charged polymer gels. The osmotic term represents the volume work against the pressure exerted by the mobile ions inside the hydrogel network. It is effectively repulsive due to the largest counterion concentration inside the gel and thus hinders the penetration of the cargo into the charged polymer network.[69] From the van't Hoff theory, the effective osmotic repulsion is given by

$$\beta u_{osm}(r) = \frac{4}{3}\pi R_c^3[\rho_+(r) + \rho_-(r) - 2\rho_s] \quad (7)$$

where R_c is the cargo radius and $4\pi R_c^3/3$ is its volume (assumed spherical). The density profiles of counterions and co-ions follow the Boltzmann distribution. For a monovalent salt they are $\rho_\pm(r) = \rho_s e^{\mp\beta e\psi(r)}$, where $\psi(r)$ is the electrostatic potential. We focus on the regime of high salt concentration, such that the Debye screening length (defined as $\kappa^{-1} = (8\pi l_B \rho_s)^{1/2}$, where l_B is the Bjerrum length) is much shorter than the thickness of the polymer shell, $\kappa^{-1} \ll b - a$. In this case, the presence of salt ions in the solution enforces overall charge neutrality, leading to a local electrostatic potential described by the Donnan potential,[70] so $\beta e\psi(r) = \ln[h(r) + \sqrt{1 + h(r)^2}]$, where $h(r) = z_m\rho_m(r)/(2\rho_s)$.

In order to deduce the expression for the steric−attractive term (second term in eq 2), we first analyze the process in the absence of short-range cargo−polymer attraction. Figure 9(a) illustrates a region

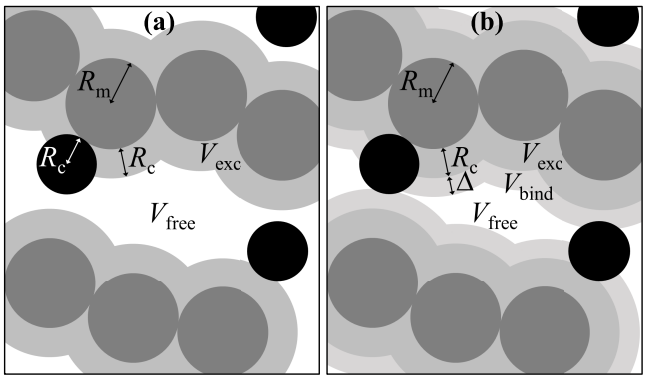

Figure 9. Illustration of the different regions inside the polymer network. Polymer chains are depicted as interconnected monomers of radius R_m (dark gray circles). Molecular cargo is modeled by spheres of radius R_c (represented by black circles). Plot (a) shows the excluded and free available volumes for neutral nonattractive cargo molecules. Plot (b) shows the excluded, binding, and free volume for neutral attractive cargo molecules.

inside the polymer network of the hydrogel. Polymer chains are formed by interconnected monomeric spherical units of radius R_m, whereas the cargo molecules are represented by spheres of radius R_c. The polymer volume fraction is given by $\phi_p = N_m V_m/V$, where N_m is the total number of monomers, $V_m = 4\pi R_m^3/3$ the volume of a monomer, and V the total volume of the polymer network. The steric exclusion partitions V in two regions: the excluded volume, V_{exc}, and the free available volume, V_{free}, where the cargo can freely move, so $V = V_{exc} + V_{free}$. Correspondingly, in terms of the volume fractions, $\phi_i = V_i/V$ and $\phi_{exc} + \phi_{free} = 1$. The expression for the excluded-volume repulsion exerted by the polymer network onto a finite-sized cargo molecule is in general complex. Fortunately, there are analytical expressions for some particular geometries, such as the Ogston formula for an assembly of randomly oriented cylindrical fibers,[36,71] for which the steric interaction is given by

https://dx.doi.org/10.1021/acsnano.0c05480
ACS Nano XXXX, XXX, XXX−XXX

$$\beta u_{ster}(r) = -\left(1 + \frac{R_c}{R_m}\right)^2 \ln(1 - \phi_p(r)) \quad (8)$$

where $\phi_p(r)$ is the polymer volume fraction at position r. Equation 8 always leads to a repulsive energy barrier that hinders the penetration of the cargo inside the hydrogel shell. Although this model assumes cargo sphericity and neglects other effects, such as dynamic fluctuations and flexibility of the polymer chains, it works fairly well on describing the excluded-volume effects in simulated polymer hydrogels.[72]

We now extend this model to include an additional short-range cargo−polymer (*e.g.*, hydrophobic) attraction. Note that various kinds of short-range attractions play a key role in many physicochemical and biological phenomena (such as protein stabilization and polymer coil-to-globule transitions)[73−76] and in the absorption of hydrophobic drugs into hydrogels containing hydrophobic polymers to serve as binding sites.[77−80] In our case, it would be responsible for the adsorption and retention of the cargo molecules at the internal surface and inside the polymer shell, respectively. Neglecting the specific details of this interaction, we introduce the following square-well pair potential, which gathers the steric exclusion and the attractive binding,

$$u_{cm}(r') = \begin{cases} \infty & r' \le R_m + R_c \\ -\epsilon & R_m + R_c < r' \le R_m + R_c + \Delta \\ 0 & r' > R_m + R_c + \Delta \end{cases} \quad (9)$$

where r' denotes the distance between the monomer and cargo centers, whereas $\epsilon > 0$ and Δ represent the characteristic strength and range of the attraction. Although the square-well potential seems to be a crude simplification, it is expected to work well for short-range interactions, given that R_c, ϵ, and Δ can be regarded as effective parameters. In fact, they can be adjusted to match the second virial coefficient of the real cargo−polymer interaction, thus providing a fair representation of the exclusion and binding effects induced by the polymer chains.

Figure 9(b) shows the three regions in which the internal volume of the polymer network partitions: excluded, binding, and free volumes, $V = V_{exc} + V_{bind} + V_{free}$, so $\phi_{exc} + \phi_{bind} + \phi_{free} = 1$. Taking into account the effect of the attraction, the effective steric−attractive interaction between a cargo molecule and the polymer network can be written as[81,82]

$$\beta u_{ster\text{-}att}(r) = -\ln(\phi_{free}(r) + \phi_{bind}(r)e^{\beta\epsilon}) \quad (10)$$

Assuming again the Ogston model for the internal morphology, we find[81,82]

$$\phi_{free}(r) = (1 - \phi_p(r))^{(1+(R_c+\Delta)/R_m)^2} \quad (11)$$

and

$$\phi_{bind}(r) = -(1 - \phi_p(r))^{(1+R_c/R_m)^2} - (1 - \phi_p(r))^{(1+(R_c+\Delta)/R_m)^2} \quad (12)$$

The resulting effective pair potential (eq 10) is shown in Figure 10 as a function of ϕ_p for different binding strengths.

To illustrate the form of $u_{ster-att}$ we use $R_m = 0.35$ nm. The cargo radius is set to $R_c = 1.25$ nm, which represents a typical value for small proteins and some drugs. The range of the attraction is set to $\Delta = 1$ nm. For $\epsilon = 0$, $u_{ster-att}$ is always repulsive due to the steric exclusion effect. For attractive wells, $\epsilon > 0$, the steric exclusion and the short-range attraction compete. For small polymer volume fractions, the attraction dominates over the steric repulsion, whereas at sufficiently large ϕ_p, the steric effect rules due to the lack of space inside the hydrogel to allocate the cargo molecules. As a result of the competition between binding attraction and steric repulsion, a minimum of $u_{ster-att}$ occurs at some intermediate polymer volume fraction, which grows with the attraction strength, ϵ. The existence of this minimum (which corresponds to a maximum of the partition coefficient, K) has been confirmed in recently reported computer simulation studies.[68,82]

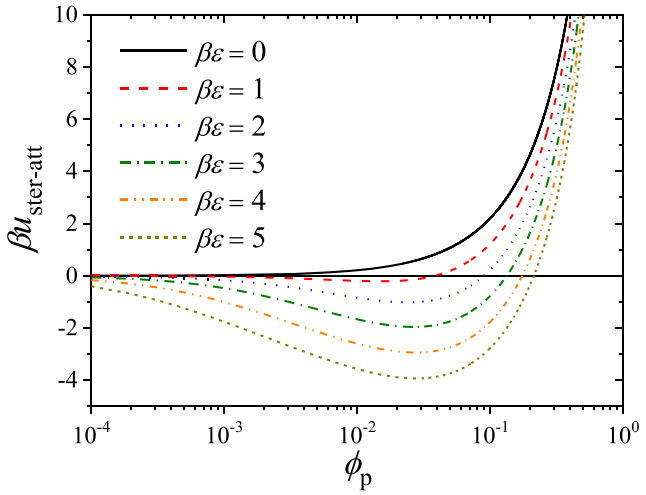

Figure 10. Steric−attractive effective pair potential (eq 10) between a neutral spherical cargo and a uniform polymer network as a function of the polymer volume fraction, ϕ_p, and the attraction strength, ϵ. The calculations were performed with $R_m = 0.35$ nm, $R_c = 1.25$ nm, and $\Delta = 1$ nm and assuming the Ogston model for the internal microstructure of the hydrogel, eqs 11 and 12

It should be emphasized that eq 10 is in fact an approximation for swollen hydrogels, where the polymer packing fraction is small. By increasing ϕ_p (for instance, upon collapsing the hydrogel), the overlapping attractions from multiple chains should be considered.[82] To correct for this reinforcing attraction effect, ϵ should be replaced by an effective density-dependent attraction $\epsilon_{eff}(\phi_p)$.

Diffusion Coefficient of Attractive Cargo inside the Polymer Network. The passive diffusive release of cargo molecules from the hollow hydrogel is controlled not only by the effective cargo−hydrogel interaction but also by the diffusion coefficient inside the polymer network. When the pore sizes of the hydrogel are comparable to the dimensions of the embedded cargo, the polymeric chains in the cross-linked network produce a steric hindrance that restricts the available volume for the cargo and increases its hydrodynamic drag. This reduces the cargo diffusion coefficient compared to the one in bulk solution. Different approximate models can be found in the literature regarding this problem.[35,83] Here, we use a heuristic expression for the diffusion coefficient that takes into account obstruction and hydrodynamic effects induced by the polymer chains:[34,36]

$$\frac{D_{ster}(r)}{D_0} = \frac{e^{-0.84\alpha(r)^{1.09}}}{1 + \sqrt{2\alpha(r)} + 2\alpha(r)/3} \quad (13)$$

where D_0 is the cargo diffusivity in the bulk solution, and $\alpha(r) \approx \beta u_{ster}(r) = -(1 + R_c/R_m)^2 \ln(1 - \phi_p(r))$. The numerator in eq 13 accounts for the steric obstruction caused by the polymers, whereas the denominator is the Brinkman equation for the hydrodynamic retardation effect.[84] This model has been previously used to investigate the encapsulation kinetics of charged molecules inside hollow hydrogels.[33] Equation 13 has been also used to fit experimental data of the diffusion coefficient of solutes inside fibrous structures, in which diffusion is controlled by steric obstruction and hydrodynamic retardation.[36] It is also consistent with recent simulation results that include hydrodynamic interactions.[85]

Note that eq 13 does not consider the existence of short-range attractive cargo−polymer interactions. To account for attractions, we write the effective diffusion coefficient inside the polymer network as $D_{eff}^* = L^2/(6\tau) \sim 1/\tau$, where $L = b - a$ is the thickness of the polymer spherical shell and τ is the typical time involved by the cargo to diffuse across it. We can split this total time into two contributions: the time involved to diffuse through the free available volume plus the time spent inside the (attractive) binding volume. By weighting these times by the corresponding volume fractions of the corresponding regions we get

https://dx.doi.org/10.1021/acsnano.0c05480
ACS Nano XXXX, XXX, XXX−XXX

$$\tau = \tau_{free}\frac{V_{free}}{V_{free} + V_{bind}} + \tau_{bind}\frac{V_{bind}}{V_{free} + V_{bind}} \quad (14)$$

The binding time, τ_{bind}, increases with the attraction strength ϵ because the adsorbed molecule needs to overcome an attractive well to escape from the binding site through the shuttling action of Brownian motion. In other words, when the cargo diffuses inside the binding volume, it is temporally retained by the attraction to specific binding sites around the polymer chains. Therefore, the binding volume can be modeled as an energy landscape consistent with consecutive attractive potential wells, with ϵ being the typical energy needed to hop from one minimum to the next one. According to Kramers, the jump frequency of this stochastic process can be written in an Arrhenius form,[56,83] so τ_{bind} and τ_{free} are related by $\tau_{bind} = \tau_{free}e^{\beta\epsilon}$. By inserting this expression into eq 14 and using $D_{eff}^* \sim \tau^{-1}$ and $\tau_{free}^{-1} \sim D_{ster}$, we obtain

$$D_{eff}^* = D_{ster}\frac{\phi_{free} + \phi_{bind}}{\phi_{free} + \phi_{bind}e^{\beta\epsilon}} \quad (15)$$

Analogously, the space-dependent diffusion coefficient $D_{eff}(r)$ for a nonuniform network can be obtained by simply inserting the expressions of $\phi_{free}(r)$ and $\phi_{bind}(r)$ given in eqs 11 and 12.

This correction to the sterically hindered diffusion coefficient (given by eq 13) implies an additional reduction of the diffusive transport provoked by the adhesion of the specific substance to the polymer chains. By taking the limit $\epsilon \to 0$ or $\Delta \to 0$ (*i.e.*, $\phi_{bind} \to 0$) we find that $D_{eff}^* \to D_{ster}$. Figure 11(a) illustrates the dependence of the cargo diffusion coefficient as a function of ϕ_p and ϵ for $R_m = 0.35$ nm, $R_c = 1.25$ nm, and $\Delta = 1$ nm. As observed, D_{eff}^* strongly decreases with the polymer volume fraction, namely, by several orders of magnitude compared to the bulk diffusion. The cargo−polymer attraction enhances this decrease even further, as the embedded molecule becomes attached to the polymer chains due to the attractive bonds.[85] This reduction of cargo mobility with the attraction can be clearly appreciated in Figure 11(b), where D_{eff}^*/D_{ster} is plotted against ϕ_p for the same set of parameters. In the limit $\phi_p \to 1$, the free available volume inside the hydrogel goes to zero much faster than the binding volume, and the effective diffusion coefficient behaves as $D_{eff}^* \approx D_{ster}e^{-\beta\epsilon}$. This scaling is in line with recent computer simulations obtained by Kim *et al.* for attractive membranes, which showed that $D_{eff}^* \sim e^{-\beta\epsilon}$ for Lennard-Jones attractions and polymer volume fractions between $\phi_p = 0.05$ and 0.42.[68] This agreement confirms that the roughness in the energy landscape inside an attractive polymer network controls the cargo diffusivity.

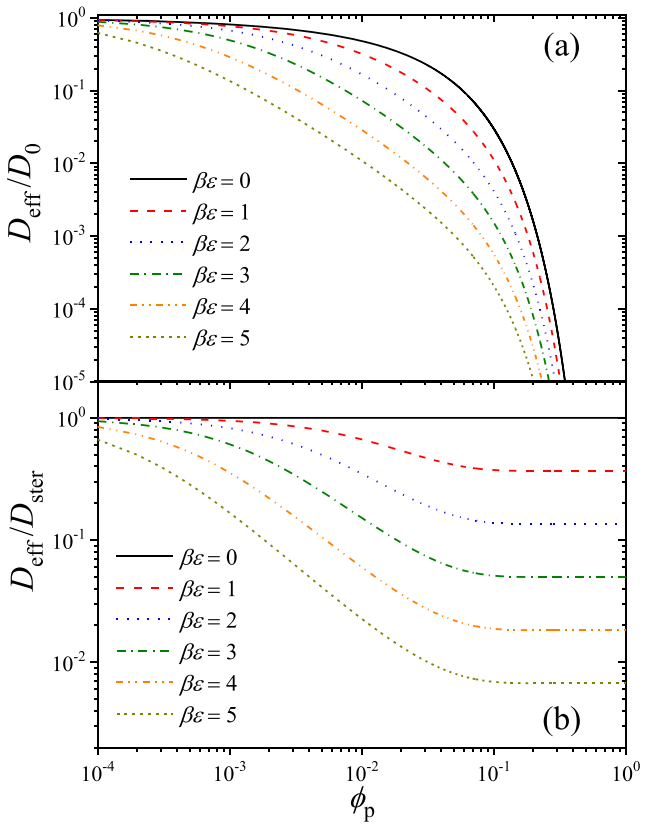

Figure 11. (a) Diffusion coefficient of the embedded cargo inside the polymer network as a function of ϕ_p, for different values of ϵ. (b) Ratio between the diffusion coefficient of attractive and non-attractive polymer shells, D_{eff}^*/D_{ster}. Calculations are performed with the same conditions as that of Figure 10.

ASSOCIATED CONTENT

Supporting Information

The Supporting Information is available free of charge at https://pubs.acs.org/doi/10.1021/acsnano.0c05480.

Part A: Calculation of the cargo time-dependent density profile using DDFT; part B: Comments on the model's assumptions (PDF)

AUTHOR INFORMATION

Corresponding Authors

Arturo Moncho-Jordá − *Departamento de Física Aplicada and Instituto Carlos I de Física Teórica y Computacional, Facultad de Ciencias, Universidad de Granada, 18071 Granada, Spain;* orcid.org/0000-0002-2001-2987; Email: moncho@ugr.es

Gerardo Odriozola − *Física de Procesos Irreversibles, Ciencias Básicas e Ingeniería, Universidad Autónoma Metropolitana-Azcapotzalco, 02200 Ciudad de México, Mexico;* orcid.org/0000-0002-0093-2129; Email: godriozo@azc.uam.mx

Authors

Ana B. Jódar-Reyes − *Departamento de Física Aplicada and Excellence Research Unit "Modeling Nature" (MNat), Universidad de Granada, 18071 Granada, Spain*

Matej Kanduč − *Jožef Stefan Institute, SI-1000 Ljubljana, Slovenia;* orcid.org/0000-0002-5307-7488

Alicia Germán-Bellod − *Departamento de Física Aplicada, Universidad de Granada, 18071 Granada, Spain*

Juan M. López-Romero − *Departamento de Química Orgánica, Facultad de Ciencias, Universidad de Málaga, 29071 Málaga, Spain*

Rafael Contreras-Cáceres − *Departamento de Química en Ciencias Farmacéuticas, Facultad de Farmacia, Universidad Complutense de Madrid, 28040 Madrid, Spain;* orcid.org/0000-0001-6313-2340

Francisco Sarabia − *Departamento de Química Orgánica, Facultad de Ciencias, Universidad de Málaga, 29071 Málaga, Spain;* orcid.org/0000-0002-5149-3576

Miguel García-Castro − *Departamento de Química Orgánica, Facultad de Ciencias, Universidad de Málaga, 29071 Málaga, Spain*

Héctor A. Pérez-Ramírez − *Física de Procesos Irreversibles, Ciencias Básicas e Ingeniería, Universidad Autónoma Metropolitana-Azcapotzalco, 02200 Ciudad de México, Mexico*

Complete contact information is available at: https://pubs.acs.org/10.1021/acsnano.0c05480

Notes

The authors declare no competing financial interest.

https://dx.doi.org/10.1021/acsnano.0c05480
ACS Nano XXXX, XXX, XXX−XXX

ACKNOWLEDGMENTS

The authors thank Professor Joachim Dzubiella (Freiburg University, Germany) and Jordi Faraudo (ICMAB Barcelona, Spain) for very helpful discussions. A.M.-J., G.O., and H.A.P.-R. acknowledge financial support from CONACyT through project A1-S-9197. A.B.J.-R. thanks the "Programa Operativo FEDER 2014-2020" and Consejería de Economía y Conocimiento de la Junta de Andalucía (project B1-FQM-112-UGR18). M.K. acknowledges the financial support from the Slovenian Research Agency (research core funding no. P1-0055). A.G-B. thanks the financial support provided by the Physics of Fluids and Biocolloids research group (FQM-115). J.M.L.-P. thanks the funding provided by Ministerio de Ciencia, Innovación y Universidades (Spain) under the project CTQ16-76311-R. R.C.-C. acknowledges funding from the Comunidad de Madrid for the "Atracción de Talento" project (2018-T1/IND-10736).

REFERENCES

(1) Tokita, M.; Tanaka, T. Friction Coefficient of Polymer Networks of Gels. *J. Chem. Phys.* **1991**, *95*, 4613−4619.

(2) Stuart, M. A. C.; Huck, W. T. S.; Genzer, J.; Müller, M.; Ober, C.; Stamm, M.; Sukhorukov, G. B.; Szleifer, I.; Tsukruk, V. V.; Urban, M.; Winnik, F.; Zauscher, S.; Luzinov, I.; Minko, S. Emerging Applications of Stimuli-Responsive Polymer Materials. *Nat. Mater.* **2010**, *9*, 101.

(3) Chen, K.; Zhou, S.; Wu, L. Self-Healing Underwater Superoleophobic and Antibiofouling Coatings Based on the Assembly of Hierarchical Microgel Spheres. *ACS Nano* **2016**, *10*, 1386−1394.

(4) Banerjee, R.; Parida, S.; Maiti, C.; Mandal, M.; Dhara, D. pH-Degradable and Thermoresponsive Water-Soluble Core Cross-Linked Polymeric Nanoparticles as Potential Drug Delivery Vehicle for Doxorubicin. *RSC Adv.* **2015**, *5*, 83565−83575.

(5) Yang, C.; Attia, A. B. E.; Tan, J. P.; Ke, X.; Gao, S.; Hedrick, J. L.; Yang, Y.-Y. The Role of Non-Covalent Interactions in Anticancer Drug Loading and Kinetic Stability of Polymeric Micelles. *Biomaterials* **2012**, *33*, 2971−2979.

(6) Wei, M.; Gao, Y.; Li, X.; Serpe, M. J. Stimuli-Responsive Polymers and their Applications. *Polym. Chem.* **2017**, *8*, 127−143.

(7) Zhao, M.; Wan, S.; Peng, X.; Zhang, B.; Pan, Q.; Li, S.; He, B.; Pu, Y. Leveraging a Polycationic Polymer to Direct Tunable Loading of an Anticancer Agent and Photosensitizer with Opposite Charges for Chemo-Photodynamic Therapy. *J. Mater. Chem. B* **2020**, *8*, 1235−1244.

(8) Dokkhan, C.; Mokhtar, M. Z.; Chen, Q.; Saunders, B. R.; Hodson, N. W.; Hamilton, B. Using Microgels to Control the Morphology and Optoelectronic Properties of Hybrid Organic-Inorganic Perovskite Films. *Phys. Chem. Chem. Phys.* **2018**, *20*, 27959−27969.

(9) Ding, T.; Baumberg, J. J. Thermo-Responsive Plasmonic Systems: Old Materials with New Applications. *Nanoscale Adv.* **2020**, *2*, 1410−1416.

(10) Kocak, G.; Tuncer, C.; Bütün, V. pH-Responsive Polymers. *Polym. Chem.* **2017**, *8*, 144−176.

(11) Wang, X.-Q.; Yang, S.; Wang, C.-F.; Chen, L.; Chen, S. Multifunctional Hydrogels with Temperature, Ion, and Magnetocaloric Stimuli-Responsive Performances. *Macromol. Rapid Commun.* **2016**, *37*, 759−768.

(12) Bertolla, M.; Cenci, L.; Anesi, A.; Ambrosi, E.; Tagliaro, F.; Vanzetti, L.; Guella, G.; Bossi, A. M. Solvent-Responsive Molecularly Imprinted Nanogels for Targeted Protein Analysis in MALDI-TOF Mass Spectrometry. *ACS Appl. Mater. Interfaces* **2017**, *9*, 6908−6915.

(13) Vinogradov, S. V. Nanogels in the Race for Drug Delivery. *Nanomedicine* **2010**, *5*, 165−168.

(14) Wu, S.; Dzubiella, J.; Kaiser, J.; Drechsler, M.; Guo, X.; Ballauff, M.; Lu, Y. Thermosensitive Au-PNIPA Yolk-Shell Nanoparticles with Tunable Selectivity for Catalysis. *Angew. Chem., Int. Ed.* **2012**, *51*, 2229−2233.

(15) Kureha, T.; Suzuki, D. Nanocomposite Microgels for the Selective Separation of Halogen Compounds from Aqueous Solution. *Langmuir* **2018**, *34*, 837−846.

(16) Pelton, R.; Chibante, P. Preparation of Aqueous Latices with N-Isopropylacrylamide. *Colloids Surf.* **1986**, *20*, 247−256.

(17) Peng, X.; Shen, J. Water-Soluble Copolymers. I. Biodegradability and Functionality of Poly[(Sodium Acrylate)-co-(4-Vinylpyridine)). *J. Appl. Polym. Sci.* **1999**, *71*, 1953−1957.

(18) Clara-Rahola, J.; Moscoso, A.; Belén Ruiz-Muelle, A.; Laurenti, M.; Formanek, P.; Lopez-Romero, J. M.; Fernández, I.; Diaz, J. F.; Rubio-Retama, J.; Fery, A.; Contreras-Cáceres, R. Au@p4VP Core@Shell pH-Sensitive Nanocomposites Suitable for Drug Entrapment. *J. Colloid Interface Sci.* **2018**, *514*, 704−714.

(19) García-Pinel, B.; Ortega-Rodríguez, A.; Porras-Alcalá, L.; Cabeza, L.; Contreras-Cáceres, R.; Ortiz, R.; Díaz, A.; Moscoso, A.; Sarabia, F.; Prados, J.; López-Romero, J. M.; Melguizo, C. Temperature-Sensitive Magnetic PNIPAM Nanosystems Loading Oxaliplatin and 5-Fluorouracil as Biocompatible Structures for Controlled Drug Delivery. *Artif. Cells, Nanomed., Biotechnol.* **2020**, *48*, 1022.

(20) Zelikin, A. N.; Li, Q.; Caruso, F. Disulfide-Stabilized Poly(Methacrylic Acid) Capsules: Formation, Cross-Linking, and Degradation Behavior. *Chem. Mater.* **2008**, *20*, 2655−2661.

(21) Levy, T.; Déjugnat, C.; Sukhorukov, G. B. Polymer Microcapsules with Carbohydrate-Sensitive Properties. *Adv. Funct. Mater.* **2008**, *18*, 1586−1594.

(22) Masoud, H.; Alexeev, A. Controlled Release of Nanoparticles and Macromolecules from Responsive Microgel Capsules. *ACS Nano* **2012**, *6*, 212−219.

(23) Kozlovskaya, V.; Alexander, J. F.; Wang, Y.; Kuncewicz, T.; Liu, X.; Godin, B.; Kharlampieva, E. Internalization of Red Blood Cell-Mimicking Hydrogel Capsules with pH-Triggered Shape Responses. *ACS Nano* **2014**, *8*, 5725−5737.

(24) McMasters, J.; Poh, S.; Lin, J. B.; Panitch, A. Delivery of Anti-Inflammatory Peptides from Hollow Pegylated Poly(nipam) Nanoparticles Reduces Inflammation in an ex Vivo Osteoarthritis Model. *J. Controlled Release* **2017**, *258*, 161−170.

(25) Qiao, Y.; He, J.; Chen, W.; Yu, Y.; Li, W.; Du, Z.; Xie, T.; Ye, Y.; Hua, S. Y.; Zhong, D.; Yao, K.; Zhou, M. Light-Activatable Synergistic Therapy of Drug-Resistant Bacteria-Infected Cutaneous Chronic Wounds and Nonhealing Keratitis by Cupriferous Hollow Nanoshells. *ACS Nano* **2020**, *14*, 3299−3315.

(26) Contreras-Cáceres, R.; Leiva, M. C.; Ortiz, R.; Díaz, A.; Perazzoli, G.; Casado-Rodríguez, M. A.; Melguizo, C.; Baeyens, J. M.; López-Romero, J. M.; Prados, J. Paclitaxel-Loaded Hollow-Poly(4-Vinylpyridine) Nanoparticles Enhance Drug Chemotherapeutic Efficacy in Lung and Breast Cancer Cell Lines. *Nano Res.* **2017**, *10*, 856−875.

(27) Li, J.; Mooney, D. J. Designing Hydrogels for Controlled Drug Delivery. *Nat. Rev. Mater.* **2016**, *1*, 16071.

(28) Korsmeyer, R. W.; Peppas, N. A. Effect of the Morphology of Hydrophilic Polymeric Matrices on the Diffusion and Release of Water Soluble Drugs. *J. Membr. Sci.* **1981**, *9*, 211−227.

(29) Lee, P. I. Modeling of Drug Release from Matrix Systems Involving Moving Boundaries: Approximate Analytical Solutions. *Int. J. Pharm.* **2011**, *418*, 18−27.

(30) Li, Y.; Zhang, Z.; van Leeuwen, H. P.; Cohen Stuart, M. A.; Norde, W.; Kleijn, J. M. Uptake and Release Kinetics of Lysozyme in and from an Oxidized Starch Polymer Microgel. *Soft Matter* **2011**, *7*, 10377−10385.

(31) Papadokostaki, K. G. Combined Experimental and Computer Simulation Study of the Kinetics of Solute Release from a Relaxing Swellable Polymer Matrix. II. Release of an Osmotically Active Solute. *J. Appl. Polym. Sci.* **2004**, *92*, 2468−2479.

(32) Angioletti-Uberti, S.; Ballauff, M.; Dzubiella, J. Dynamic Density Functional Theory of Protein Adsorption on Polymer-Coated Nanoparticles. *Soft Matter* **2014**, *10*, 7932−7945.

(33) Moncho-Jordá, A.; Germán-Bellod, A.; Angioletti-Uberti, S.; Adroher-Benítez, I.; Dzubiella, J. Nonequilibrium Uptake Kinetics of Molecular Cargo into Hollow Hydrogels Tuned by Electrosteric Interactions. *ACS Nano* **2019**, *13*, 1603−1616.

https://dx.doi.org/10.1021/acsnano.0c05480
ACS Nano XXXX, XXX, XXX−XXX

(34) Johnson, E. M.; Berk, D. A.; Jain, R. K.; Deen, W. M. Hindered Diffusion in Agarose Gels: Test of Effective Medium Model. *Biophys. J.* **1996**, *70*, 1017−23.
(35) Amsden, B. Solute Diffusion within Hydrogels. Mechanisms and Models. *Macromolecules* **1998**, *31*, 8382−8395.
(36) Bosma, J.; Wesselingh, J. Partitioning and Diffusion of Large Molecules in Fibrous Structures. *J. Chromatogr., Biomed. Appl.* **2000**, *743*, 169−180.
(37) Xing, Z.; Wang, C.; Yan, J.; Zhang, L.; Li, L.; Zha, L. Dual Stimuli Responsive Hollow Nanogels with IPN Structure for Temperature Controlling Drug Loading and pH Triggering Drug Release. *Soft Matter* **2011**, *7*, 7992−7997.
(38) Rodríguez-Ropero, F.; van der Vegt, N. F. A. Direct Osmolyte-Macromolecule Interactions Confer Entropic Stability to Folded States. *J. Phys. Chem. B* **2014**, *118*, 7327−7334.
(39) Sheybanifard, M.; Beztsinna, N.; Bagheri, M.; Buhl, E. M.; Bresseleers, J.; Varela-Moreira, A.; Shi, Y.; van Nostrum, C. F.; van der Pluijm, G.; Storm, G.; Hennink, W. E.; Lammers, T.; Metselaar, J. M. Systematic Evaluation of Design Features Enables Efficient Selection of Π Electron-Stabilized Polymeric Micelles. *Int. J. Pharm.* **2020**, *584*, 119409.
(40) Deutch, J. M. A. Simple Method for Determining the Mean Passage Time for Diffusion Controlled Processes. *J. Chem. Phys.* **1980**, *73*, 4700−4701.
(41) Takeuchi, H. A Jump Motion of Small Molecules in Glassy Polymers: A Molecular Dynamics Simulation. *J. Chem. Phys.* **1990**, *93*, 2062−2067.
(42) Müller-Plathe, F. Diffusion of Penetrants in Amorphous Polymers: A Molecular Dynamics Study. *J. Chem. Phys.* **1991**, *94*, 3192−3199.
(43) Sok, R. M.; Berendsen, H. J. C.; van Gunsteren, W. F. Molecular Dynamics Simulation of the Transport of Small Molecules across a Polymer Membrane. *J. Chem. Phys.* **1992**, *96*, 4699−4704.
(44) Pérez-Fuentes, L.; Drummond, C.; Faraudo, J.; Bastos-González, D. Anions Make the Difference: Insights from the Interaction of Big Cations and Anions with Poly(N-Isopropylacrylamide) Chains and Microgels. *Soft Matter* **2015**, *11*, 5077−5086.
(45) Kanduč, M.; Kim, W. K.; Roa, R.; Dzubiella, J. Transfer Free Energies and Partitioning of Small Molecules in Collapsed PNIPAM Polymers. *J. Phys. Chem. B* **2019**, *123*, 720−728.
(46) Berndt, I.; Pedersen, J. S.; Richtering, W. Structure of Multiresponsive "Intelligent" Core-Shell Microgels. *J. Am. Chem. Soc.* **2005**, *127*, 9372−9373.
(47) Adroher-Benítez, I.; Ahualli, S.; Martín-Molina, A.; Quesada-Pérez, M.; Moncho-Jordá, A. Role of Steric Interactions on the Ionic Permeation Inside Charged Microgels: Theory and Simulations. *Macromolecules* **2015**, *48*, 4645−4656.
(48) Moncho-Jordá, A.; Quesada-Pérez, M. Crossover of the Effective Charge in Ionic Thermoresponsive Hydrogel Particles. *Phys. Rev. E: Stat. Phys., Plasmas, Fluids, Relat. Interdiscip. Top.* **2019**, *100*, 050602.
(49) Wischke, C.; Schwendeman, S. P. Principles of Encapsulating Hydrophobic Drugs in PLA/PLGA Microparticles. *Int. J. Pharm.* **2008**, *364*, 298−327. Future Perspectives in Pharmaceutics Contributions from Younger Scientists.
(50) Kim, C. K.; Ghosh, P.; Pagliuca, C.; Zhu, Z.-J.; Menichetti, S.; Rotello, V. M. Entrapment of Hydrophobic Drugs in Nanoparticle Monolayers with Efficient Release into Cancer Cells. *J. Am. Chem. Soc.* **2009**, *131*, 1360−1361.
(51) Dursch, T. J.; Taylor, N. O.; Liu, D. E.; Wu, R. Y.; Prausnitz, J. M.; Radke, C. J. Water-Soluble Drug Partitioning and Adsorption in HEMA/MAA Hydrogels. *Biomaterials* **2014**, *35*, 620−629.
(52) Marconi, U. M. B.; Tarazona, P. Dynamic Density Functional Theory of Fluids. *J. Chem. Phys.* **1999**, *110*, 8032−8044.
(53) Klein, G.; Born, M. Mean First-Passage Times of Brownian Motion and Related Problems. *P. R. Soc. A-Math. Phys.* **1952**, *211*, 431−443.
(54) Ansari, A. Mean First Passage Time Solution of the Smoluchowski Equation: Application to Relaxation Dynamics in Myoglobin. *J. Chem. Phys.* **2000**, *112*, 2516−2522.
(55) Amato, D. V.; Lee, H.; Werner, J. G.; Weitz, D. A.; Patton, D. L. Functional Microcapsules via Thiol-Ene Photopolymerization in Droplet-Based Microfluidics. *ACS Appl. Mater. Interfaces* **2017**, *9*, 3288−3293.
(56) Kramers, H. Brownian Motion in a Field of Force and the Diffusion Model of Chemical Reactions. *Physica* **1940**, *7*, 284−304.
(57) Lonsdale, H.; Merten, U.; Riley, R. Transport Properties of Cellulose Acetate Osmotic Membranes. *J. Appl. Polym. Sci.* **1965**, *9*, 1341−1362.
(58) Paul, D. R. The Solution-Diffusion Model for Swollen Membranes. *Sep. Purif. Methods* **1976**, *5*, 33−50.
(59) Palasis, M.; Gehrke, S. H. Permeability of Responsive Poly (N-Isopropylacrylamide) Gel to Solutes. *J. Controlled Release* **1992**, *18*, 1−11.
(60) Wijmans, J. G.; Baker, R. W. The Solution-Diffusion Model: A Review. *J. Membr. Sci.* **1995**, *107*, 1−21.
(61) Matsuyama, H.; Teramoto, M.; Urano, H. Analysis of Solute Diffusion in Poly(Vinyl Alcohol) Hydrogel Membrane. *J. Membr. Sci.* **1997**, *126*, 151−160.
(62) Huang, X.; Margulis, C. J.; Berne, B. J. Dewetting-Induced Collapse of Hydrophobic Particles. *Proc. Natl. Acad. Sci. U. S. A.* **2003**, *100*, 11953−11958.
(63) Sharma, S.; Debenedetti, P. G. Evaporation Rate of Water in Hydrophobic Confinement. *Proc. Natl. Acad. Sci. U. S. A.* **2012**, *109*, 4365−4370.
(64) Weaver, B. A. How Taxol/Paclitaxel Kills Cancer Cells. *Mol. Biol. Cell* **2014**, *25*, 2677−2681.
(65) Cremasco, M. A.; Wang, L. N.-H. Estimation of Partition, Free and Specific Diffusion Coefficients of Paclitaxel and Taxanes in a Fixed Bed by Moment Analysis: Experimental, Modeling and Simulation Studies. *Acta Sci., Technol.* **2012**, *34*, 33−40.
(66) Ohshima, H. Electrophoresis of Soft Particles: Analytic Approximations. *Electrophoresis* **2006**, *27*, 526−533.
(67) Yu, H.; Li, D.; Xu, F.; Liu, B.; Chen, C. Effect of Solvent Water Molecules on Human Serum Albumin Complex-Docked Paclitaxel by MM-PBSA Method. *Interdiscip. Sci.: Comput. Life Sci.* **2017**, *9*, 205−213.
(68) Kim, W. K.; Chudoba, R.; Milster, S.; Roa, R.; Kanduč, M.; Dzubiella, J. Tuning the Selective Permeability of Polydisperse Polymer Networks. *Soft Matter* **2020**, *14*, 8144−8154.
(69) Adroher-Benítez, I.; Moncho-Jordá, A.; Dzubiella, J. Sorption and Spatial Distribution of Protein Globules in Charged Hydrogel Particles. *Langmuir* **2017**, *33*, 4567−4577.
(70) Yigit, C.; Welsch, N.; Ballauff, M.; Dzubiella, J. Protein Sorption to Charged Microgels: Characterizing Binding Isotherms and Driving Forces. *Langmuir* **2012**, *28*, 14373−14385.
(71) Ogston, A. G. The Spaces in a Uniform Random Suspension of Fibres. *Trans. Faraday Soc.* **1958**, *54*, 1754−1757.
(72) Ahualli, S.; Martín-Molina, A.; Quesada-Pérez, M. Excluded Volume Effects on Ionic Partitioning in Gels and Microgels: A Simulation Study. *Phys. Chem. Chem. Phys.* **2014**, *16*, 25483−25491.
(73) Sarkar, M.; Li, C.; Pielak, G. J. Soft Interactions and Crowding. *Biophys. Rev.* **2013**, *5*, 187−194.
(74) Mukherji, D.; Wagner, M.; Watson, M. D.; Winzen, S.; de Oliveira, T. E.; Marques, C. M.; Kremer, K. Relating Side Chain Organization of PNIPAm with its Conformation in Aqueous Methanol. *Soft Matter* **2016**, *12*, 7995−8003.
(75) Sapir, L.; Harries, D. Macromolecular Compaction by Mixed Solutions: Bridging versus Depletion Attraction. *Curr. Opin. Colloid Interface Sci.* **2016**, *22*, 80−87.
(76) Nayar, D.; Folberth, A.; van der Vegt, N. F. A. Molecular Origin of Urea Driven Hydrophobic Polymer Collapse and Unfolding Depending on Side Chain Chemistry. *Phys. Chem. Chem. Phys.* **2017**, *19*, 18156−18161.
(77) Thatiparti, T. R.; Shoffstall, A. J.; von Recum, H. A. Cyclodextrin-Based Device Coatings for Affinity-Based Release of Antibiotics. *Biomaterials* **2010**, *31*, 2335−2347.
(78) Soukasene, S.; Toft, D. J.; Moyer, T. J.; Lu, H.; Lee, H.-K.; Standley, S. M.; Cryns, V. L.; Stupp, S. I. Antitumor Activity of Peptide

https://dx.doi.org/10.1021/acsnano.0c05480
ACS Nano XXXX, XXX, XXX−XXX

Amphiphile Nanofiber-Encapsulated Camptothecin. *ACS Nano* **2011**, *5*, 9113−9121.
(79) Zhang, P.; Cheetham, A. G.; Lin, Y.-a.; Cui, H. Self-Assembled Tat Nanofibers as Effective Drug Carrier and Transporter. *ACS Nano* **2013**, *7*, 5965−5977.
(80) Mateen, R.; Hoare, T. Injectable, in Situ Gelling, Cyclodextrin-Dextran Hydrogels for the Partitioning-Driven Release of Hydrophobic Drugs. *J. Mater. Chem. B* **2014**, *2*, 5157−5167.
(81) Moncho-Jordá, A.; Adroher-Benítez, I. Ion Permeation inside Microgel Particles Induced by Specific Interactions: From Charge Inversion to Overcharging. *Soft Matter* **2014**, *10*, 5810−5823.
(82) Pérez-Mas, L.; Martín-Molina, A.; Quesada-Pérez, M.; Moncho-Jordá, A. Maximizing the Absorption of Small Cosolutes inside Neutral Hydrogels: Steric Exclusion versus Hydrophobic Adhesion. *Phys. Chem. Chem. Phys.* **2018**, *20*, 2814−2825.
(83) Masaro, L.; Zhu, X. Physical Models of Diffusion for Polymer Solutions, Gels and Solids. *Prog. Polym. Sci.* **1999**, *24*, 731−775.
(84) Brinkman, H. A. Calculation of the Viscous Force Exerted by a Flowing Fluid on a Dense Swarm of Particles. *Flow, Turbul. Combust.* **1949**, *1*, 27−34.
(85) Hansing, J.; Netz, R. R. Hydrodynamic Effects on Particle Diffusion in Polymeric Hydrogels with Steric and Electrostatic Particle-Gel Interactions. *Macromolecules* **2018**, *51*, 7608−7620.

https://dx.doi.org/10.1021/acsnano.0c05480
ACS Nano XXXX, XXX, XXX−XXX